Traffic Injury Prevention, 4:240–248, 2003

ISSN: 1538-9588 print / 1538-957X online
DOI: 10.1080/15389580390216244

A New Laboratory Rig for Evaluating Helmets Subject to Oblique Impacts

MAGNUS AARE and PETER HALLDIN

Division of Neuronic Engineering, Department of Aeronautical and Vehicle Engineering, Royal Institute of Technology, Stockholm, Sweden

Current requirements and regulations governing motorcycle helmets around the world are based on test results of purely radial impacts, which are statistically rare in real accidents. This study presents a new impact rig for subjecting test helmets to oblique impacts, which therefore is able to test impacts of increased statistical relevance to real motorcycle accidents. A number of different head-helmet interfaces have been investigated. A test rig was constructed to produce oblique impacts to helmets simulating those occurring in real motorcycle accidents. A Hybrid III dummy head was fitted with accelerometers to measure the accelerations arising during impact testing. The equipment used for data collection was validated in both translational and rotational acceleration. In order to better resemble the human head, an artificial scalp was fitted to the hybrid dummy. The same test rig was used to investigate the performance of a number of different helmets. Impact velocities ranging from 7.3 to 9.9 m/s were tested using a number of different impact angles and impact areas. This study shows that the new test rig can be used to provide useful data at speeds of up to 50 km/h and with impact angles varying from purely tangential to purely radial. The rotational accelerations observed differ greatly depending on both helmet and scalp designs. For example, a helmet with a sliding outer shell placed on an experimental head fitted with an artificial scalp (made to resemble the human scalp) reduces rotational accelerations of the head by up to 56%, compared with those of an experimental head fitted with a fixed scalp and conventional helmet. The degree of slippage between the skull and the scalp, and between the scalp and the helmet, leads to considerable variation in the results. This innovative test rig appears to provide an accurate method for measuring accelerations in an oblique impact to a helmet. In order to obtain a good level of repeatability in oblique impact testing, it is crucial that the helmet be fixed to the head in the exact same way in each individual test. Both the position and the angle of impact must be reproduced identically in each test. The test rig used here has shown that this type of rig can be used to compare different helmet designs, and it therefore is able to contribute to achieving safer helmets.

Keywords Helmet Test; Oblique Impact; Rotational Acceleration

About 6,000 people are killed in Europe each year in accidents involving motorized two-wheeled vehicles (International Road Traffic and Accident Database, 2000). The costs facing European societies are enormous, not only in relation to the years of life lost in fatalities but also the costs for rehabilitating the injured. The most frequently occurring injuries resulting from motorcycle accidents are injuries to the head. Therefore, the wearing of adequate head protection is of great importance in the prevention of these injuries. Contemporary safety helmets are based on well-proven, but conservative, designs. This is not due to conservatism of the helmet manufacturers, but rather it is due to aging test regulations.

It is well known that motorcycle accidents can occur across an infinite range of directions and speeds. Using statistics from 253 accidents from three different countries, Otte and coresearchers (1999) have shown that the average speed involved in a motorcycle accident is 44 km/h, and that the average angle of the body to the ground or to the side of a car at impact is 28°. The frontal and temporal regions of the head are the most common areas of impact. This is indicated by damage to helmets. Areas close to the visor attachment points—at the sides of the helmet—were damaged in 18% of accidents, while the chin guard was fractured in 15% of accidents.

Rotational acceleration of the head is caused mainly by tangential force, which is the most common injury-causing pattern of force in bicycle and motorcycle crashes (Mills & Gilchrist, 1997). Only those impacts directed straight toward the center of gravity of an object can be considered to be radial; all others are oblique or tangential. As purely radial impacts are rare in reality, rotational accelerations almost always occur. Gennarelli (1983) described the most frequently occurring injuries sustained in motor vehicle accidents that lead to long-term rehabilitation or death, including for example subdural hematomas

Received 12 September 2002; accepted 20 March 2003.
Address correspondence to Magnus Aare, Department of Aeronautical and Vehicle Engineering, Royal Institute of Technology (KTH), SE-100 44, Stockholm, Sweden. E-mail: aare@kth.se

(SDHs) and diffuse axonal injuries (DAIs). These findings were subsequently confirmed by Aare and von Holst (2003). SDHs are caused by ruptures to either an artery or a bridging vein, whereas DAIs are caused by disruptions to axons in the brain tissue. Gennarelli concluded that SDHs were generated by short-duration, high-amplitude rotational acceleration, whereas DAIs were generated by longer-duration, lower-amplitude rotational acceleration. Margulies and Thibault (1992) proposed that the onset of DAIs occurs at an angular acceleration of 10 krad/s^2 in combination with a change in rotational velocity of 100 rad/s.

Motorcycle helmets currently are tested primarily for translational acceleration. In a conventional helmet test (such as the ECE22.05), an experimental aluminum head is fitted with sensors and placed in a helmet. The helmet-head system is dropped onto various surfaces and the acceleration recordings are compared with guidelines in the relevant legislation. Indeed, all the relevant regulations and standards are based on drop tests. Thus, the test procedures used today result in helmets that protect the head effectively against radial impacts, while the level of protection against oblique impacts remains unknown.

Halldin (2001) presented the results of helmets subjected to oblique impact testing (see Figure 1). Halldin's results showed that it was possible to reduce rotational acceleration by up to 39% with a new type of helmet design, without changing the desirable energy-absorbing properties observed in purely radial impacts. However, the equipment used by Halldin was not able to generate a speed of more than 30 km/h. Moreover, rotational accelerations were measurable around only one axis at a time.

In the tests presented by Halldin (2001), the artificial head fitted very well into the test helmet. Because the human scalp is not attached to the head in a single fixed position, Halldin pointed out the merits of conducting tests using an artificial scalp. A wig had been used in the British Standard BS6658, testing the efficiency of helmet retention systems, but the scalp had been fixed to the head in one position. Only one relevant reference could be found in the literature on the characteristics of the human scalp, and that was Gambarotta et al. (2002).

The aim of this study has been to calibrate and evaluate a test rig for investigating oblique impacts on various helmet designs and head-scalp interfaces.

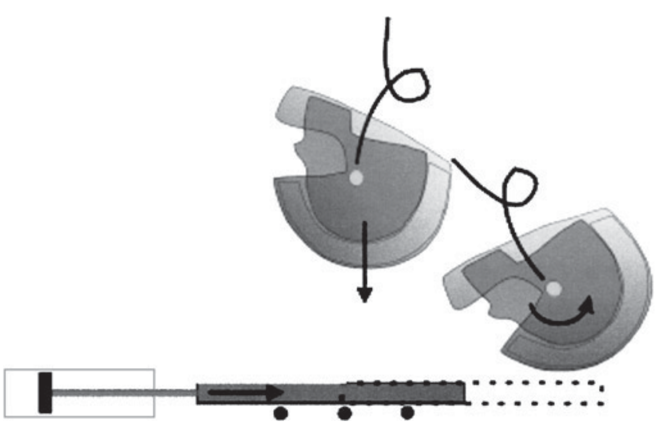

Figure 1 The oblique impact test.

MATERIALS AND METHODS

The Oblique Impact Test Rig

The basic objective of the test rig described here was to introduce tangential force into helmet testing. Impacts in motorcycle accidents are rarely fully radial; instead they most often are oblique (Otte et al., 1999). An oblique force is the result of both radial and tangential components. The tangential component induces rotational acceleration in the head.

Figure 2 presents a photographic overview of the helmet test rig. This type of test rig was first presented by Harrison et al. (1996), and again by Halldin (2001). Figure 2 shows the Hybrid III dummy head (1) inside a helmet (2), positioned within a frame (3). The frame was attached to two pillars (4) and was able to travel in a vertical direction with almost negligible friction. The helmet strike plate (5) moved horizontally along two Teflon-coated rails (6). The strike plate (weighing 12.1 kg) was accelerated using a pneumatic cylinder (7). Compressed air used to drive the rig was stored in a tank (8), and was introduced into the cylinder via a valve (9). The pressure in the tank could be adjusted with a regulator (10). Speeds of up to 10 m/s (36 km/h) could be achieved in both horizontal and vertical directions, allowing impact speeds of up to 14 m/s (50 km/h) to be reached. Sensors were mounted on the rails for measuring the velocity of the plate before and after the helmet impacts. Similar velocimeters were mounted on the pillars to measure the vertical speed of the falling frame.

The Experimental Head

The artificial head used in this study was a Hybrid III crash test dummy head. A system of nine accelerometers was mounted inside the test head (see Figure 2) according to the 3-2-2-2 method described by Padgaonkar et al. (1975). Using this method it is possible to measure the linear accelerations in all directions, and the rotational accelerations around all axes. The distance between the accelerometers in this system varied between 31 and 32 mm. All the data obtained from the accelerometers were stored in a computer. The equipment used in this study did not strictly follow the recommendations of the Society of Automotive Engineers standard SAE J211, because SAE J211 does not differentiate between rotational and translational accelerations. The equipment used here is described further below.

The nine accelerometers had a range of 500 g and were manufactured by Dytran Instruments, Inc. Four of these nine were model 3032A and the rest were model 3015. These two models have identical characteristics, the difference being that 3032A is a later version of 3015 made by the same manufacturer. The nine accelerometers were controlled by five IOtech DBK4 two-channel dynamic signal input cards, which also collected the data from the accelerometers. The accelerometer samples were obtained at a frequency of 20 kHz. The data were collected using a DAQ board 2000 card housed in the computer. This card had

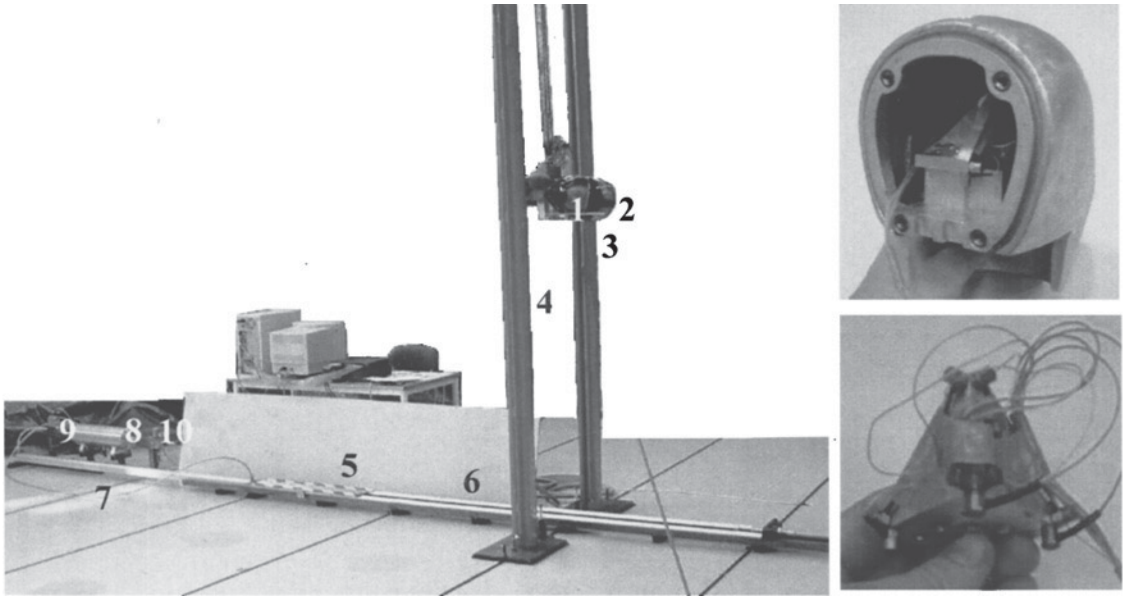

Figure 2 The test rig (left) and 3-2-2-2 system (right), where (1) is the Hybrid III dummy head, (2) is the helmet, (3) the frame, (4) the mounting pillars, (5) the helmet strike plate, (6) the Teflon-coated rails, (7) the pneumatic cylinder, (8) the compressed air tank, (9) the cylinder valve, and (10) the regulator.

a resolution of 2^{16} levels. All the collected data were filtered using an IOtech DBK4 12-pole Butterworth low-pass filter. Different cut-off frequencies were tested, and 281 Hz was found to be optimal for this application. LabView software was used to develop the computer code at the Royal Institute of Technology (KTH), Stockholm. The accelerometer system was validated for both translation and rotation (see the Appendix).

The Test Helmets

Two different types of helmets were tested, though both had the same type of shell (ABS thermoplastic) and liner (expanded polystyrene (EPS) 40 kg/m^3). These were exactly the same types of helmets as those studied by Halldin (2001). Helmet types have been referred to as: (1) glued, because the shell has been glued to the liner (typical of most conventional helmets); and (2) multidirectional impact protection system (MIPS), featuring a shell separated from the liner by a low-friction layer (see Figure 3a). The low-friction layer in this helmet is made of Teflon, and attached to the outside of the liner. This layer enables the shell to move a certain distance (represented by s in Figure 3b). This distance can attain a maximum of 2 cm after a tangential or oblique force has been applied to the outer shell. The weights and moments of inertia for the two types of helmet tested have been presented in Table I. The moments of inertia were computed after timing the oscillation period on a rotating table containing the helmets. The elastic rubber joint (see Figure 3a) is responsible for the major part of the weight difference between the two helmet types, as the Teflon in the MIPS helmet weighs only about as much as the glue used in the glued helmet. No effort has been undertaken by us to reduce the weight of the MIPS helmet.

No comfort foam padding, which exhibits a high coefficient of friction (approximately 0.4) was used between the head and the liner in any of the helmets.

The Artificial Scalp

An artificial scalp has been used to simulate the movement of the human scalp relative to the cranium (see Figure 3c). This artificial scalp was constructed using two rubber bathing caps with a section of medicine ball sandwiched between them. A thin layer of oil was introduced between the inner cap and the section of medicine ball in order to reduce friction (see Figure 3b). The original artificial skin on the dummy head was removed before attaching the artificial scalp to the dummy's head. It should be pointed out here that this device is only a very coarse approximation of the human scalp, specifically designed to be incorporated into testing two different helmet designs in a more human-like simulation.

The human scalp can slide approximately 10 mm in relation to the underlying human cranium (Gambarotta et al., 2002). In

Table I Moments of inertia and masses of experimental heads and helmets

	Moment of inertia (kg cm^2)			
	Ear-to-ear	Nose-to-rear	Top-to-neck	Mass (g)
Experimental head with fixed scalp	197	141	165	3,488
Experimental head with artificial scalp	194	146	170	3,472
Glued helmet	78	74	84	850
MIPS helmet	105	100	108	1,030

Abbreviation: MIPS, multidirectional impact protection system.

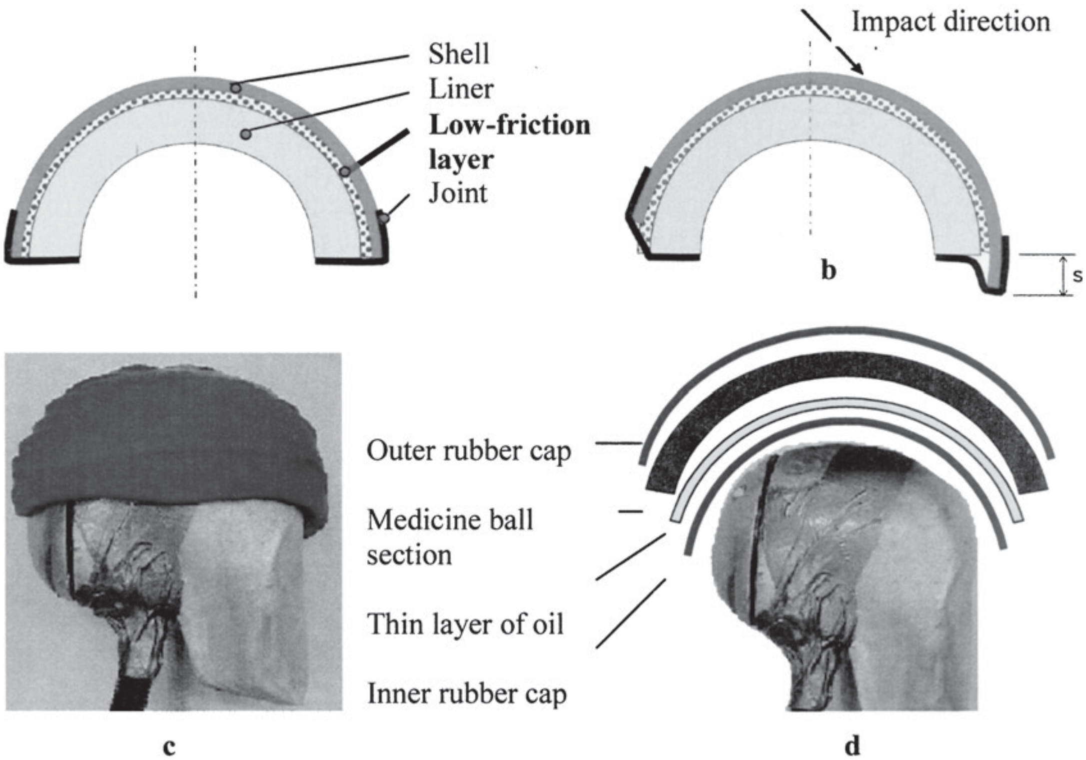

Figure 3 (a) Representative cross section through the MIPS helmet, (b) representation of the MIPS helmet during impact, (c) picture of the artificial scalp, and (d) representation of the structure of the artificial scalp.

order to mimic this, the artificial scalp was held in position with strips of duct tape with 10 mm slack. The artificial scalp was validated against tests conducted on a human volunteer.

The moment of inertia was measured using the original experimental head, and the experimental head fitted with the artificial scalp (see Table I). The same method was used as for measuring the moment of inertia on the helmets (the rotation table method).

Test Procedure

Experimental impacts were performed in three different areas and directions (see Figure 4). Each helmet was subject to one impact only at each impact site, and no more than three times in total. The impact plate was covered with grinding paper to simulate an asphalt surface. The coefficient of friction between the helmet shell and the plate was measured as 0.5. The test head was fixed firmly enough in the helmets so that no chin strap was necessary. The impact tests were carried out using the following four speeds and angles:

1. 7.3 m/s at 45°, where 0° is purely tangential and 90° is purely radial
2. 9.9 m/s at 45°
3. 9.7 m/s at 31°
4. 4.9 m/s at 90°

All the tests were filmed with a high-speed camera to make sure that the position of the helmet remained correct throughout the fall, and to photodocument the impacts.

Some additional impact tests were performed on impact areas designated 2 and 3, where the fit of the helmet to the head was improved by attaching wedges of EPS between the head and the helmet.

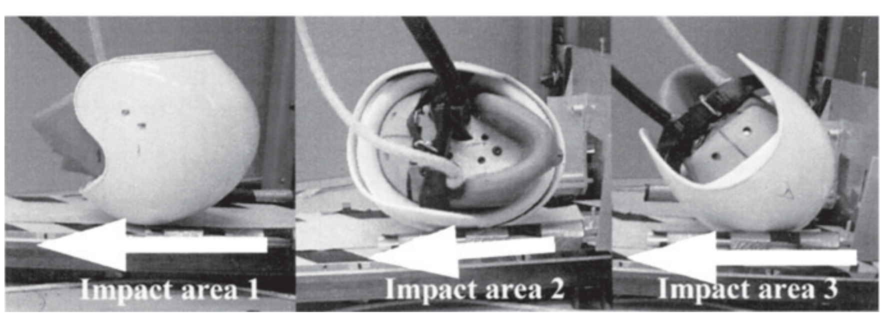

Figure 4 The three different impact orientations.

Table II Impact test descriptions and results

Type of helmet	Type of scalp	Impact speed (m/s)	Impact angle	Maximum rotational acceleration (krad/s^2)[a]	Duration of rotational acceleration (msea)[a]	Translational acceleration (g)[a]	Rotational velocity change (rad/s)[a]	No. of tests
Impact area 1								
Glued	Fixed	7.3	45°	7.83–8.66 (8.19)	7.1–7.8 (7.4)	139–151 (143)	26.4–32.0 (29.3)	3
MIPS	Fixed	7.3	45°	5.01–5.52 (5.23)	8.1–8.8 (8.5)	121–141 (130)	23.3–23.6 (23.5)	3
Glued	Artificial	7.3	45°	3.73–4.85 (4.30)	9.9–11.3 (10.8)	109–148 (132)	22.5–25.3 (24.1)	3
MIPS	Artificial	7.3	45°	3.18–4.35 (3.59)	9.2–11.0 (10.3)	78–144 (121)	19.6–22.0 (20.9)	3
Glued[b]	Fixed	9.9	45°	10.6–11.7 (11.0)	4.6–6.9 (5.57)	192–226 (208)	29.8–38.3 (34.9)	3
MIPS	Fixed	9.9	45°	5.60–7.14 (6.29)	8.5–10.2 (9.3)	213–241 (229)	29.0–32.5 (30.7)	3
Glued	Fixed	9.7	31°	11.9–12.4 (12.2)	7.1–7.5 (7.3)	146–169 (155)	44.2–44.7 (44.5)	3
MIPS	Fixed	9.7	31°	7.06–7.42 (7.24)	9.5–10.1 (9.8)	161–163 (162)	33.7–34.3 (34.0)	3
Impact area 2								
Glued	Fixed	7.3	45°	9.68–12.2 (10.6)	6.5–6.7 (6.6)	136–146 (140)	31.4–39.6 (34.3)	3
MIPS	Fixed	7.3	45°	9.38–10.7 (10.0)	7.1–7.3 (7.2)	137–149 (141)	33.6–37.3 (35.3)	3
Glued	Artificial	7.3	45°	8.35–8.87 (8.70)	7.3–7.8 (7.5)	126–145 (138)	30.1–32.7 (31.6)	3
MIPS	Artificial	7.3	45°	6.76–9.43 (8.21)	7.2–7.3 (7.2)	120–141 (129)	24.3–33.2 (28.7)	3
Glued, improved it with wedges	Fixed	7.3	45°	11.4–12.7 (12.1)	6.5–6.9 (6.7)	155–163 (160)	37.6–40.7 (38.7)	3
Impact area 3								
Glued	Fixed	7.3	45°	7.60–8.68 (8.01)	6.5–7.3 (6.7)	187–200 (193)	23.5–29.9 (25.7)	3
MIPS	Fixed	7.3	45°	4.33–6.20 (5.55)	3.1–6.5 (5.3)	149–165 (156)	11.7–20.3 (15.1)	3
Glued	Artificial	7.3	45°	4.66–6.16 (5.28)	6.5–8.6 (7.4)	157–193 (170)	14.6–17.0 (15.8)	3
MIPS	Artificial	7.3	45°	4.09–5.17 (4.75)	6.6–8.3 (7.3)	97–137 (119)	13.8–18.0 (16.0)	3
Glued, improved it with wedges	Fixed	7.3	45°	7.25–7.74 (7.57)	4.4–4.7 (4.5)	148–208 (183)	21.9–27.8 (24.4)	3
Impact at the top of the head								
Glued	Fixed	4.9	90°	—	—	154–166 (161)	—	3
MIPS	Fixed	4.9	90°	—	—	152–166 (157)	—	3

Abbreviation: MIPS, multidirectional impact protection system.
[a]Range (average).
[b]The liner broke in two of three tests.

RESULTS

The accelerometer system was validated first; the results of which have been presented in the Appendix. Validation of the translational accelerations showed that the accelerometers recorded almost exactly the same values as the real accelerations. Validation of the rotational accelerations showed errors of just a few percent. This error was due mainly to inaccurate measurements of the oscillation amplitudes, and vibrations in the tripod on which the axis was mounted.

The results of the impact tests are presented in Table II, which includes peak rotational acceleration, the duration of rotational acceleration, translational acceleration, and the change in rotational velocity. It can be seen in this table that, compared with the glued helmet, the MIPS helmet led to a reduction in the rotational accelerations in all types of impacts. The rotational velocities were also reduced in most impact cases, but not by as much as were the rotational accelerations. It can also be seen from the same table that the artificial scalp reduced the effects of impacts significantly more than the fixed scalp.

Typical characteristics of the rotational accelerations observed have been plotted in Figure 5, where each curve represents the average of three impact tests. Table III presents a comparison of the peak rotational acceleration for the two helmet types, and two scalp configurations studied. The loss of the impact plate velocity due to the impact of the helmet varied from 1.1 m/s to 1.4 m/s, depending on the speed immediately prior to impact.

Measurements of tests featuring the artificial scalp were validated against corresponding measurements using a human volunteer. An "off-the-shelf" helmet was positioned firmly enough on the volunteer's head to be able to neglect the effects of comfort foam deformation and slippage between the volunteer's scalp and the helmet. Gradually loading more and more weights to the front of the helmet shell—just in front of the volunteer's

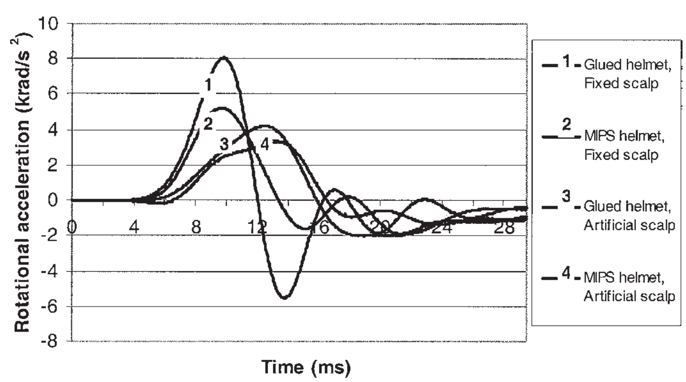

Figure 5 Rotational acceleration curves for the impact area designated 1 with an impact speed of 7.3 m/s (note that each curve is the average of three impact tests).

Table III Reductions in rotational acceleration presented as percentages

	Impact speed (m/s)	Impact angle	Case	Reduction in rotational acceleration (%)
Impact area 1				
Glued helmet	7.3	45°	Artificial scalp compared to fixed scalp	47
MIPS helmet	7.3	45°	Artificial scalp compared to fixed scalp	31
Fixed scalp	7.3	45°	MIPS compared to glued	36
Artificial scalp	7.3	45°	MIPS compared to glued	17
Fixed scalp	9.9	45°	MIPS compared to glued[a]	43
Fixed scalp	9.7	31°	MIPS compared to glued	41
Impact area 2				
Glued helmet	7.3	45°	Artificial scalp compared to fixed scalp[b]	28
MIPS helmet	7.3	45°	Artificial scalp compared to fixed scalp[b]	18
Fixed scalp	7.3	45°	MIPS compared to glued[b]	17
Artificial scalp	7.3	45°	MIPS compared to glued[b]	6
Impact area 3				
Glued helmet	7.3	45°	Artificial scalp compared to fixed scalp	34
MIPS helmet	7.3	45°	Artificial scalp compared to fixed scalp	14
Fixed scalp	7.3	45°	MIPS compared to glued	31
Artificial scalp	7.3	45°	MIPS compared to glued	10

Abbreviation: MIPS, multidirectional impact protection system.
[a]The liner broke in two of three tests.
[b]The head came loose inside the helmet due to the helmet deformation.

forehead—allowed observation of any movement of the scalp (and consequently also of the helmet) at a force of about 15 N. Movement of a distance of about 10 mm in a downward direction was observed at the front of the helmet in this setup, which agrees with the findings of Gambarotta and colleagues (2002). This 10 mm displacement remained until the force was removed and the helmet reverted to its original position. The same procedure was then used with the artificial scalp on the experimental head. The artificial scalp also moved with a loading of about 15 N applied to the front of the helmet. The main difference between the behaviors of the human scalp and the artificial scalp was that the artificial scalp did not return to its original position when the force was removed.

DISCUSSION

The results of the tests performed in this study show good agreement with previous research carried out by Halldin (2001). This study has investigated three main objects: (1) a new oblique impact test rig, (2) a new helmet design, and (3) an artificial scalp.

The Oblique Impact Test Rig

The test rig presented here proved to be a useful tool for investigating oblique impacts and optimizing helmets to suit realistic impacts. The test results represent a variety of different loading levels and impact situations. This is important because helmets are not symmetrical in all directions, leading to variations in impact in real crashes. Consequently, it is important to test a particular helmet using a variety of impact sites and angles.

Some difficulties have been experienced attempting to achieve exactly the same impact speed in any two tests due to variations, for example, in the friction between the impact plate and the rails, and in air pressure. These variations, however, were within a range of just a few percent. An alternative could have been to drop the helmet onto an anvil, as in BS6658; however, the drop tower would have had to be made much higher in order to reach the same impact speeds as the test rig presented in this article. Another limitation with the test method presented here (and indeed with most helmet test methods) is that only the head of the test dummy is used. A more realistic simulation probably would involve using a whole dummy, or at least the head, neck, and torso. This would change the dynamics of the impact, and would decrease the rotational accelerations experienced by the dummy head, since the boundary conditions for the head would change. However, the Hybrid III dummy neck probably would be a bit too stiff for this purpose. The use of a rigid head in testing should also to be discussed. This has been considered by Willinger and Kopp (1993). The human head might not behave in a rigid fashion when it comes to high-speed impacts, because: (a) it deforms, and (b) there is interaction between the brain and the head that cannot be achieved with a rigid experimental head.

The Helmets

Because the moment of inertia is higher for this version of the MIPS helmet than the glued helmet, this raises the question of whether or not it is the MIPS system (the sliding outer shell) or the higher inertia that reduces the rotational accelerations. The moment (M) was the same in two similar tests, independent of which helmet was used. According to Eq. (1), the angular (rotational) acceleration ($\ddot{\theta}$) is therefore linearly dependent on the moment of inertia (I) in the system—in this case the combination of the head and the helmet.

$$M = \ddot{\theta} \cdot I \tag{1}$$

However, it should be mentioned that because the artificial scalp and the shell of the MIPS helmet move during impact, and the dummy skin and the helmets deform during impact, the values presented in Table I are only approximations and consequently might change during an impact. Using Eq. (1) and the values presented in Table I, it becomes clear that the MIPS accounts for the bulk of the rotational acceleration reduction, which was 30% in the impact area designated 1, 9% in 2, and 18% in 3. Overall, the linear accelerations were independent of helmet type. The reason for the lower peak rotational accelerations in the MIPS helmet is the damping effect of the sliding outer shell. Both the low-friction layer and the joint in this helmet type absorb energy, which accounts for the main differences in the results between the two helmet types.

In Table II, it can be seen that the change in rotational velocity generally decreases in magnitude as the rotational acceleration decreases and the pulse duration increases. Therefore, the change in rotational velocity does not decrease to the same extent as do the rotational accelerations.

As discussed, the MIPS helmet reduces the rotational accelerations and the change in rotational velocities. It is, however, difficult to say how this influences the human brain. A literature survey has shown that the following parameters are important when predicting head injuries, such as DAI and SDH, from oblique impacts: rotational acceleration, change in rotational velocity, and pulse duration (Holbourn, 1943; Margulies & Thibault, 1992; Ommaya et al., 1967). DiMasi and colleagues (1995) and Ueno and Melvin (1995) pointed out that the combination of rotational and translational accelerations is important. A decreased rotational acceleration and a decreased change in rotational velocity causes a decrease in shear strain and shear deformation in brain tissue, which has important implications for the prevention of injuries such as SDH and DAI (Margulies & Thibault, 1992).

In the high-speed movies taken of the impact area designated 2, it could be seen that helmet deformation resulted in the helmet fitting more loosely around the experimental head. This provides a plausible explanation for the large variation observed in the rotational accelerations, and why the impact area designated 2 showed little reduction in rotational acceleration with the MIPS helmet. Additional tests were performed with EPS wedges attached to the helmet to achieve a better fit between the experimental head and the helmets, in order to overcome these problems. This resulted in improved repeatability, and the variations in the results were halved. These wedges also improved the beneficial effects of the MIPS. The same technique was applied to the impact area designated 3, which exhibited the same improvement in the variation. The loosened fit probably would not be as pronounced in a real helmet, as the comfort foam helps keep the head and helmet in a fixed position relative to each other. It is important to make sure that the helmet is fixed to the experimental head in the same way in all tests. This could be a problem, however, when testing helmets with different inner geometries. When it comes to measuring rotations, how well the head fits the helmet is crucial. However, one way to control the interface between the experimental head and the liner is to pressurize the "skin" of the experimental head forcing it against the helmet. This can be done with small air bags placed between the aluminum part of the experimental head and skin. These air bags can be pumped up to expand the experimental head inside the helmet before each impact.

These preliminary results, comparing different helmet designs, illustrate possibilities for significantly reducing the rotational accelerations and the change of rotational velocity experienced by both the experimental head with an artificial scalp and one with a fixed scalp.

Tests have also been conducted on off-the-shelf, full-face helmets. Some of these helmets featured the MIPS. These tests showed results similar to those presented above (note that they are not yet comprehensive enough to be presented in a scientific paper but their augmentation is planned in the future).

The Artificial Scalp

The experimental head used in this study has been fitted with an artificial scalp to better resemble the human head. However, identical reconstruction of the artificial scalp after each test session may be problematic. Validation of the artificial scalp presented in the Results section was a very coarse procedure, with the objective of ensuring an approximate resemblance to the human scalp. If an artificial scalp is going to be used in deriving a rigorous standard, then it is crucial that some simple validation step be used to ensure identical scalp characteristics after each test session.

Arguments exist both for and against using an artificial scalp in a test standard. The best solution probably would be to use a fixed scalp, while also adjusting injury thresholds. Because an artificial scalp decreases rotational accelerations, the threshold can be set slightly higher when a fixed scalp is used in equivalent test situations.

CONCLUSIONS

It has become necessary to improve current but outmoded helmet-testing regulations, as the current standard test procedures do not adequately represent real motorcycle accidents. This study presents a new test rig as one possible way of testing helmets in a more realistic manner.

When testing more than one impact scenario, it is important to control the experimental head and helmet interface in order to minimize variation, and thereby increase reliability and comparability. This is particularly important in tests that include rotations.

It is possible to achieve new and improved helmet designs that decrease rotational accelerations markedly, without negatively affecting their proven desirable performance in radial impacts. An example of this is the MIPS helmet, which appears to reduce rotational accelerations and rotational velocities in all impact situations tested. However, the magnitude of the reduction effect in the MIPS helmet is somewhat decreased in tests incorporating an artificial scalp. Importantly though, some difficulties have been experienced in trying to achieve an artificial scalp that exhibits exactly the same characteristics each test session. This problem has yet to be solved. An artificial scalp may not be necessary in oblique impact tests, if the injury thresholds are adjusted to take the effect of the scalp into account.

ACKNOWLEDGMENTS

The authors wish to thank Länsförsäkringar Corporation Research Fund for their financial support. We would also like to thank the staff members at the Department of Aeronautical and Vehicle Engineering, at the Royal Institute of Technology (KTH), Stockholm, Sweden, for their valuable guidance and assistance.

REFERENCES

Aare, M., von Holst, H. (2003) Injuries from Motorcycle and Moped Crashes in Sweden from 1987 to 1999, *Inj. Control Safety Promotion*, Vol. 10, pp. 131–138.

DiMasi, F. P., Eppinger, R. H., Bandak F. A. (1995) Computational Analysis of Head Impact Response under Car Crash Loadings, *39th Stapp Car Crash Conf.*, pp. 425–438.

Gambarotta, L., Massabo, R., Morbiducci, R. (2002) A Computational Model of Scalp Skin for In Vivo Material Characterization and Reconstructive Surgery Simulation, *Proc. 5th World Cong. Computational Mechanics.*

Gennarelli, T. A. (1983) Head Injury in Man and Experimental Animals: Clinical Aspects, *Acta Neurochirurgica*, Suppl. 32, pp. 1–13.

Halldin, P. (2001) *Prevention and Prediction of Head and Neck Injury in Traffic Accidents—Using Experimental and Numerical Methods*, Report 2001-1, Department of Aeronautics, Royal Institute of Technology, Stockholm, Sweden.

Harrison, T. I., Mills, N. J., Turner, M. S. (1996) Jockeys' Head Injuries and Skullcap Performance, *Proc. 23rd IRCOBI Conf.*, pp. 49–62.

Holbourn, A. H. S. (1943) Mechanics of Head Injury, *Lancet*, Vol. 2, pp. 438–441.

International Road Traffic and Accident Database. (2000) Available at http://www.bast.de/htdocs/fachthemen/irtad/english/englisch.html, Aceessed 10 March 2002.

Margulies, S. S., Thibault, L. E. (1992) A Proposed Tolerance Criterion for Diffuse Axonal Injuries in Man, *J. Biomech.*, Vol. 32, pp. 917–923.

Mills, N. J., Gilchrist, A. (1997) Response of Helmets in Direct and Oblique Impacts, *International Journal of Crashworthiness*, Vol. 2, pp. 7–23.

Ommaya, A. K., Yarnell, P., Hirsch, A. E., Harris A. E. (1967) Scaling of Experimental Data on Cerebral Concussion in Sub-Human Primates to Concussion Threshold for Man, *11th Stapp Car Crash Conf.*, pp. 73–80.

Otte, D., Chinn, B., Doyle, D., Mäkitupa, S., Sturrock, K. Schuller, E. (1999) *Contribution to Final Report of COST 327 Project*, University of Hannover, Hannover, Germany.

Padgaonkar, A. J., Krieger, K. W., King, A. I. (1975) Measurement of Angular Acceleration of a Rigid Body Using Linear Accelerometers, *J. Appl. Mechanics*, Vol. 42, pp. 552–556.

Ueno, K., Melvin, J. W. (1995) Finite Element Model Study of Head Impact Based on Hybrid III Head Acceleration: The Effects of Rotational and Translational Acceleration, *J. Biomech. Eng.*, Vol. 117, pp. 319–328.

Willinger, R., Kopp, C. M. (1993) Proposition of a New Dummy Head: The Bimass 150 Principle, *Proc. 20th IRCOBI Conf.*, pp. 229–240.

APPENDIX

Validation

Validation was performed to ensure that the accelerometer system was set up correctly. The system was validated for both translation and rotation. For translational validation, the accelerometer system was placed on an oscillator and the acceleration calculated according to the following:

$$a = (2\pi \cdot f)^2 \cdot A \cdot \cos(2\pi \cdot f \cdot t) \qquad (2)$$

where

a = acceleration
f = frequency of the oscillation
A = amplitude of the oscillation
t = time

The frequency used for validation was 50 Hz and the amplitude 3.0 mm. This in turn gives an acceleration of 296 m/s^2. The 3-2-2-2 system showed an acceleration of 296 ± 3 m/s^2, depending on the direction.

The same oscillator was used to calibrate the accelerometer system for rotational acceleration. The oscillator was attached to an arm mounted on an axis. The oscillator was used to induce rotation of the axis. The accelerometer system was mounted on top of the rotating axis. Equation 3 below describes the rotational acceleration of the arm in the validation set up.

$$\ddot{\alpha} = (2\pi \cdot f)^2 \cdot \frac{A}{2L} \cdot \cos(2\pi \cdot f \cdot t) \qquad (3)$$

where

$\ddot{\alpha}$ = rotational acceleration
f = frequency of the oscillation
A = amplitude of the oscillation
L = the length of the arm
t = time

The frequency used for this calibration was 40 Hz, and the amplitude 2.0 mm. This in turn gives a rotational acceleration of 647 rad/s^2. The 3-2-2-2 system showed a rotational acceleration of 640 ± 30 rad/s^2 depending on the axis. The errors and variations arose mainly due to inaccurate oscillation amplitude measurements, and vibrations in the tripod on which the axis was attached.

Calculation of Rotational Acceleration

The 3-2-2-2 system registers rotational accelerations around three axes. However the maximum rotational acceleration does not normally occur exactly around one of these axes. One way of measuring the rotational acceleration is to calculate the resultant acceleration at each moment in time. One disadvantage with this method is that the negative response or "recoil" of the rotational acceleration curve cannot be seen, since the sum of the quadratic is never negative.

Rotational accelerations were calculated in this study by introducing a fictitious axis into the coordinate system used for the head. The direction chosen for the fictitious axis is the direction in which the resultant rotational acceleration is at a maximum. The rotational acceleration around this axis is then derived at each moment. This makes it possible to measure the duration of the positive contribution to the rotational acceleration.